Title

Non-viral Gene Therapy for Stargardt Disease with ECO/pRHO-ABCA4 Self-Assembled Nanoparticles

Journal

Molecular Therapy, 28(1)

ISSN

1525-0016

Authors

Sun, Da
Schur, Rebecca M
Sears, Avery E
et al.

Publication Date

2020

DOI

10.1016/j.ymthe.2019.09.010

Peer reviewed

Molecular Therapy
Original Article

Non-viral Gene Therapy for Stargardt Disease with ECO/*pRHO-ABCA4* Self-Assembled Nanoparticles

Da Sun,[1,3] Rebecca M. Schur,[1,3] Avery E. Sears,[2,4] Song-Qi Gao,[1] Amita Vaidya,[1] Wenyu Sun,[1] Akiko Maeda,[2] Timothy Kern,[2,4] Krzysztof Palczewski,[2,4] and Zheng-Rong Lu[1]

[1]Department of Biomedical Engineering, Case Western Reserve University, Cleveland, OH 44106, USA; [2]Department of Pharmacology, Case Western Reserve University, Cleveland, OH 44106, USA

Stargardt disease (STGD) is an autosomal recessive retinal disorder caused by a monogenic *ABCA4* mutation. Currently, there is no effective therapy to cure Stargardt disease. The replacement of mutated *ABCA4* with a functional gene remains an attractive strategy. In this study, we have developed a non-viral gene therapy using nanoparticles self-assembled by a multifunctional pH-sensitive amino lipid ECO and a therapeutic *ABCA4* plasmid. The nanoparticles mediated efficient intracellular gene transduction in wild-type (WT) and *Abca4*$^{-/-}$ mice. Specific ABCA4 expression in the outer segment of photoreceptors was achieved by incorporating a rhodopsin promoter into the plasmids. The ECO/*pRHO-ABCA4* nanoparticles induced substantial and specific *ABCA4* expression for at least 8 months, 35% reduction in A2E accumulation on average, and a delayed Stargardt disease progression for at least 6 months in *Abca4*$^{-/-}$ mice. ECO/plasmid nanoparticles constitute a promising non-viral gene therapy platform for Stargardt disease and other visual dystrophies.

INTRODUCTION

Stargardt disease (STGD) is characterized as a gradual bilateral decline in central vision and visual acuity that begins in adolescence.[1,2] It is commonly caused by mutations in the *ABCA4* gene, which encodes a 210-kDa ATP-dependent flippase importer. ABCA4 flips the orientation of membrane-bound lipids from the luminal leaflet of the outer segment disc membrane to the cytosolic side, and it transports both phosphatidylethanolamine (PE) and the all-*trans*-retinal (atRAL)/PE Schiff base (*N*-Ret-PE) into the cytosol, where atRAL is converted to all-*trans*-retinol (atROL) by retinol dehydrogenase RDH8 and RDH12.[3,4] The functional loss of ABCA4 results in the accumulation of photo-toxin *N*-retinylidene-*N*-retinyl ethanolamine bisretinoid (A2E) in retinal pigmented epithelium (RPE) phagosomes as well as lipofuscin buildup and, eventually, irreversible retinal degeneration.[5]

Stargardt disease occurs in approximately 1/8,000–1/10,000 individuals. Currently, there is no effective therapy approved to cure the disease. Therapeutics and treatment strategies, such as deuterated vitamin A, stem cell therapy, and modulation of the complement system, have been developed and tested to prevent excessive lipofuscin accumulation and to rescue the phenotype of Stargardt disease.[6–9] Although these therapeutics have demonstrated promise in slowing Stargardt disease progression, there is still a long way to go to accomplish clinical translation.

Gene therapy represents a promising prophylactic treatment of monogenic retinal disorders, including Stargardt disease. In gene therapy, a healthy copy of the mutated gene is delivered into the relevant cells, where it relies on the endogenous translational machinery to synthesize the normal protein and restore normal function. Recently, the adeno-associated virus (AAV), specifically of the AAV2 serotype, has been approved for treating Leber's congenital amaurosis.[10–12] Unfortunately, standard AAV2 vectors cannot be directly expanded for treating Stargardt disease, due to their limited cargo capacity for the large *ABCA4* gene. Dual-AAV strategies and lentiviruses have been tested to address the limitation of AAV-based gene therapy for Stargardt disease and Usher Syndrome.[13–16] However, limited progress has been achieved for clinical translation. Compared with most viral vectors, non-viral gene delivery systems have larger packaging capacity, are flexible in application, and safe to use.[17–19] Gene therapy with non-viral delivery systems could be a promising approach for treating Stargardt disease.

Previously, we developed a multifunctional pH-sensitive amino lipid (1-aminoethyl)iminobis[N-(oleoylcysteinyl-1-amino-ethyl)propionamide) (ECO) (Figure 1A) for efficient intracellular delivery of therapeutic nucleic acids.[20,21] ECO self-assembles with nucleic

Received 25 April 2019; accepted 6 September 2019;
https://doi.org/10.1016/j.ymthe.2019.09.010.

[3]These authors contributed equally to this work.

[4]Present address: Gavin Herbert Eye Institute, Department of Ophthalmology and Department of Physiology and Biophysics, University of California, Irvine, Irvine, CA 92697, USA

Correspondence: Zheng-Rong Lu, PhD, Department of Biomedical Engineering, Case Western Reserve University, Wickenden 427, Mail Stop 7207, 10900 Euclid Avenue, Cleveland, OH 44106, USA.
E-mail: zxl125@case.edu

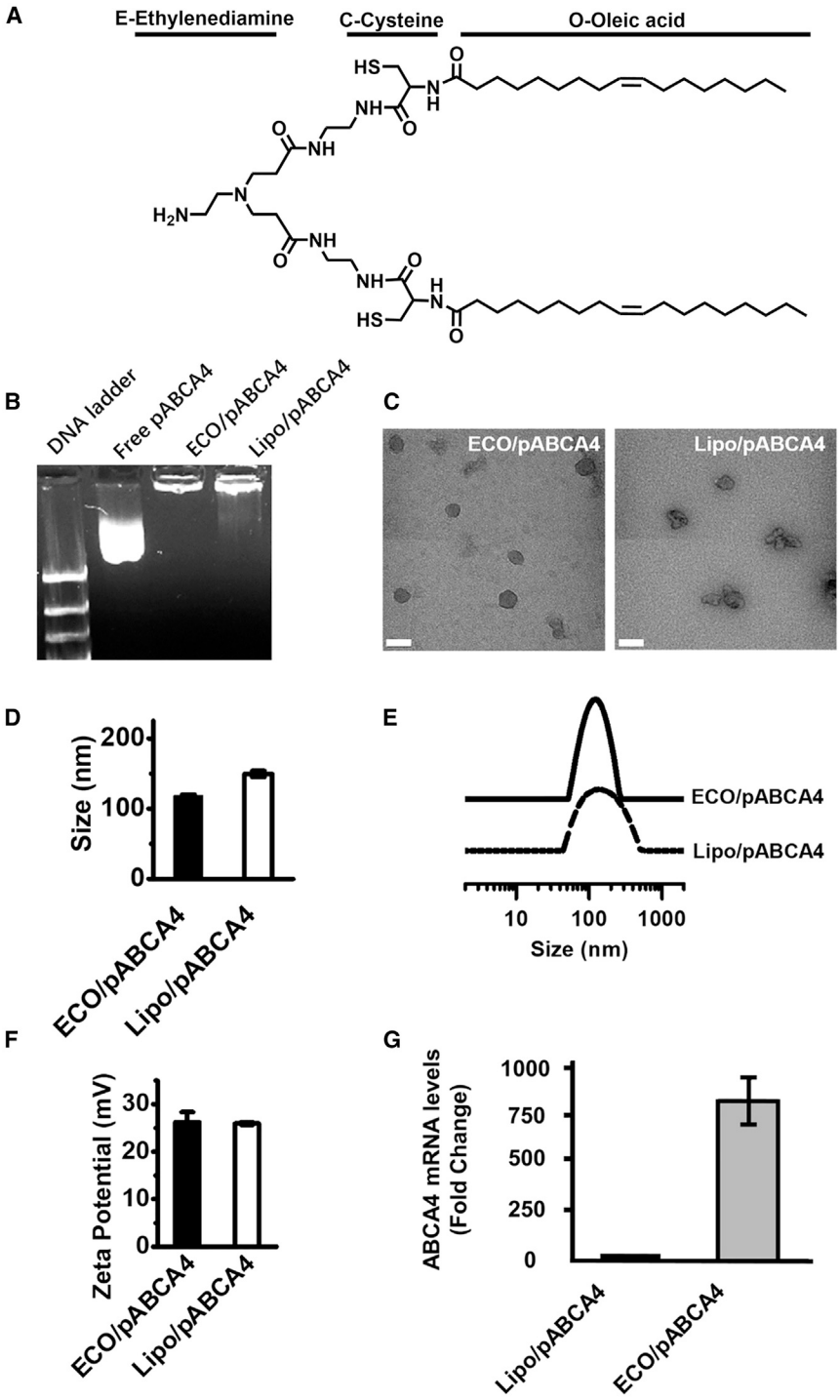

Figure 1. Formulation and Characterization of ECO/*pCMV-ABCA4* Nanoparticles with Lipofectamine as Control

(A–F) ECO structure (A), agarose gel electrophoresis (B), and transmission electron microscopy (C), DLS measurements of nanoparticle size (D), size distribution (E), zeta potential (F), and *ABCA4* mRNA expression levels in ARPE-19 cells (G) of the nanoparticles. (DLS measurements were performed at particle counts from 150~400 kcounts/s. Relative frequency intensity weighted nanoparticle size distribution and zeta potential were recorded. Scale bar represents 100 nm. Statistical analysis was conducted with two-tailed Student's t test. $^{**}p < 0.05$.)

acids of various sizes to form stable nanoparticles, and it facilitates pH-sensitive amphiphilic endosomal escape and reductive cytosolic release (PERC) of nucleic acids in target tissues.[19–25] In this study, we developed self-assembled nanoparticles of ECO and an *ABCA4* plasmid modified with a bovine rhodopsin promoter (RHO) (ECO/*pRHO-ABCA4*) to induce specific gene expression in the photoreceptors, with the goal of treating Stargardt disease.[26] The efficacy and safety of ECO/*pRHO-ABCA4* nanoparticle-based gene replacement therapy were evaluated by the subretinal administration in *Abca4*$^{-/-}$ mice, an orthologous rodent model to human Stargardt disease.

RESULTS

ECO readily forms stable nanoparticles with the large *pABCA4* plasmid by self-assembly at an amine/phosphate (N/P) ratio of 10. We characterized the DNA encapsulation, morphology, size, surface charge, and *in vitro* transfection efficiency of ECO/*pABCA4* with Lipofectamine (Lipo/*pABCA4*) as a control. Gel electrophoresis showed complete encapsulation of cytomegalovirus promoter (*pCMV*)-*ABCA4* (16 kb) with ECO, while DNA smears were seen for Lipo/*pCMV-ABCA4*, indicating less of the shielding effect of the DNA cargo (Figure 1B). ECO/*pCMV-ABCA4* and Lipo/*pCMV-ABCA4* nanoparticles had a size of around 100 nm, as shown by transmission electron microscopy, and a hydrodynamic diameter of 118.0 ± 1.8 nm and 149.5 ± 4.3 nm, respectively, by dynamic light scattering. ECO/*pCMV-ABCA4* demonstrated less particle aggregation and a better uniformity with narrower particle size distribution than Lipo/*pCMV-ABCA4* (Figures 1C and 1E). ECO/*pCMV-ABCA4* and Lipo/*pCMV-ABCA4* exhibited positive zeta potentials of 26.3 ± 2.1 mV and 26.0 ± 0.3 mV, respectively. *In vitro* transfection in ARPE-19 cells showed that ECO/*pCMV-ABCA4* resulted in about an 800-fold higher mRNA expression of *ABCA4* than Lipo/*pCMV-ABCA4*, determined by qRT-PCR (Figure 1G). In addition, ECO/*pCMV-ABCA4* exhibited much lower cytotoxicity than Lipo/*pCMV-ABCA4* (Figure S1). Our findings demonstrated that ECO forms

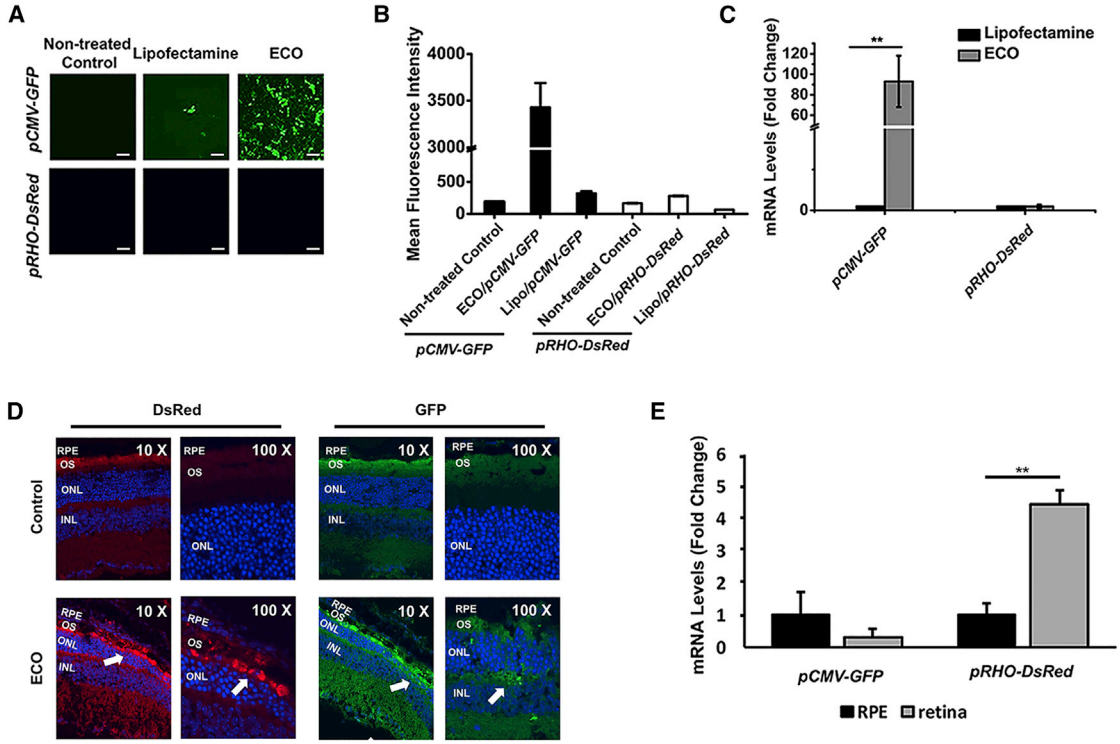

Figure 2. *In Vitro* and *In Vivo* Photoreceptor-Specific Gene Expression Using ECO/*pRHO-DNA* Nanoparticles

(A–E) Confocal images (A), quantification by flow cytometry of mean fluorescence intensities (B), and mRNA levels by qRT-PCR (C) of reporter gene expression in ARPE-19 cells mediated by ECO/*pRHO-DsRed* and ECO/*pCMV-GFP* 48 h after transfection; immunofluorescence confocal images of retinal tissue (D) and mRNA levels (E) of *GFP* and *DsRed* expression induced by CMV and RHO promoters in 129S1/SvImJ mice 3 days after subretinal injection with non-treated eyes as controls (n = 3). Statistical analysis was conducted with two-tailed Student's t test. **$p < 0.05$. Scale bars represent 100 μm.

stable nanoparticles with the large *pCMV-ABCA4*, which demonstrated narrow size distribution and mediated highly efficient transfection with low cytotoxicity.

Effective gene therapy of Stargardt disease requires specific expression of the *ABCA4* gene in the outer segment (OS) after efficient delivery into photoreceptor cells.[27,28] To achieve photoreceptor-specific expression of *ABCA4*, a RHO promoter was cloned into the therapeutic *ABCA4* plasmid. We evaluated RHO-induced specific gene expression using reporter plasmids, a common cytomegalovirus (CMV) promoter-driven *GFP* (*pCMV-GFP*), and a bovine rhodopsin promoter-driven *DsRed* (*pRHO-DsRed*) in ARPE-19 cells and wild-type mice. Strong GFP expression in ARPE-19 cells transfected by ECO/*pCMV-GFP* was displayed by fluorescence confocal microscopy, flow cytometry, and qPCR, while a much lower *DsRed* expression was detected in cells transfected with ECO/*pRHO-DsRed* (Figures 2A–2C and S2). ECO/*pCMV-GFP* resulted in a 93-fold increase in mRNA expression of *GFP* as compared with a Lipofectamine control (Lipo/*pCMV-GFP*), as shown by qRT-PCR (Figure 2C). Both ECO and Lipofectamine facilitated the same low-level expression of *DsRed*, due to the ineffectiveness of the RHO promoter in the ARPE-19 cells.

We next evaluated the efficiency of photoreceptor-specific expression with the RHO promoter by co-injecting ECO/*pCMV-GFP* and ECO/*pRHO-DsRed* nanoparticles subretinally in wild-type 129S1/SvImJ mice at a 1:1 ratio. The mice were euthanized 3 days later, and fluorescence immunohistochemistry revealed that both GFP and DsRed were expressed in the photoreceptor segments (Figure 2D). GFP expression was also observed in the outer plexiform layer, but DsRed was not. Higher expression of *DsRed* in the retina than the RPE was verified, based on mRNA levels (Figure 2E). The results indicated photoreceptor-specific gene expression induced by the RHO promoter.

A photoreceptor-specific plasmid *pRHO-ABCA4* was constructed using molecular cloning to insert the *ABCA4* gene into the backbone of the *DsRed* reporter plasmid containing the RHO region (Figures 3, S3, and S4). Agarose gel electrophoresis verified that *ABCA4* retained its size without extraneous digestion and the *DsRed* gene (0.7 kb) was successfully removed from the plasmid backbone (5.4 kb) (Figure 3A). Ligation of the two purified restriction fragments was again verified by gel electrophoresis by comparing with ligase-free and single-component controls (Figure 3B). Self-ligation of *ABCA4* was observed as two additional bands appeared when the ligase was present (lane 4). When both DNA fragments and the

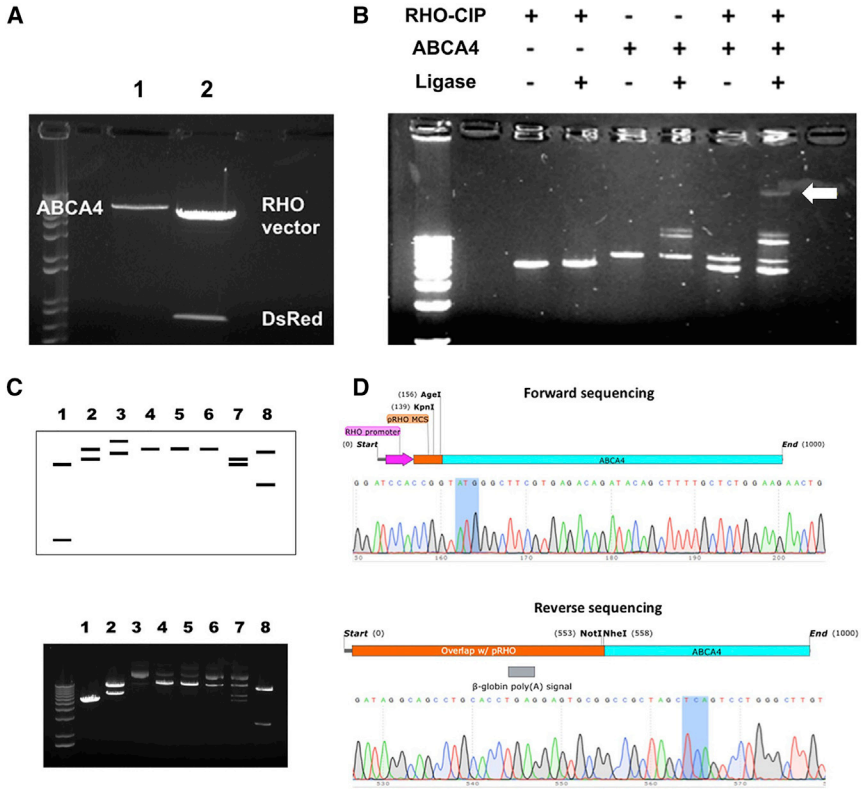

Figure 3. Design, Development, and Verification of *pRHO-ABCA4* Plasmid Construct

(A) DNA fragments following restriction digest at NheI and NotI sites. Lane 1, PCR-amplified *ABCA4*; lane 2, *pRHO-DsRed* incubated with calf intestinal alkaline phosphatase during digestion. (B) Ligation reaction products of the *RHO* vector with *ABCA4* and appropriate controls. The final lane contains the reaction with the final ligated product (white arrow). (C) Verification of plasmid construction by restriction digestion. Predicted (top) and experimental (bottom) gel electrophoresis of *pRHO-ABCA4* and parent plasmids following endonuclease digestion at the restriction sites. Lane 1, *pRHO-DsRed* at NheI/AgeI; lane 2, *pCEP4-ABCA4* at NheI/AgeI; lane 3, *pRHO-ABCA4*; lane 4, *pRHO-ABCA4* at AgeI; lane 5, *pRHO-ABCA4* at NotI; lane 6, *pRHO-ABCA4* at NheI; lane 7, *pRHO-ABCA4* at NheI/AgeI; lane 8, *pRHO-ABCA4* at KpnI. (D) Verification of plasmid construction by Sanger sequencing in the forward (top) and reverse (bottom) directions. Start and stop codons are highlighted in gray. Overlap with the *pRHO* vector is shown in orange and purple. Overlap with the *ABCA4* gene is shown in blue.

ligase were included in the reaction, 5 bands were present (lane 6). Four of these bands corresponded to the controls, including the linear *RHO* vector, the linear *ABCA4* fragment, and the *ABCA4* self-ligation products. The fifth band with the slowest migration and a larger size than the individual components was reasoned to be the desired ligation product. The final plasmid construct was confirmed by a restriction digest at various restriction sites followed by gel electrophoresis to verify the predicted sizes that were anticipated after endonuclease cutting (Figure 3C).

Reasonable correlation was achieved between the predicted and observed gel electrophoresis of *pRHO-ABCA4* after endonuclease digestion at the restriction sites. Extra bands in the experimental gel electrophoresis were likely due to incomplete digestion of the circular plasmid during the endonuclease reaction, as verified by the size correlation between the upper bands and the uncut circular *pRHO-ABCA4* plasmid (lane 3). Sanger sequencing further validated successful insertion of the *ABCA4* gene into the *pRHO* vector (Figure 3D). Sequencing was performed in the forward direction using the sequencing primer for the bovine RHO promoter region and in the reverse direction from the M13 rev primer site. Sequencing results were aligned with the plasmid maps from *pRHO-DsRed* and the cDNA sequence for human *ABCA4* (NCBI: NM_000350.2), which was also shown in the Supplemental Results. The full *ABCA4* gene sequence was further verified by sequencing, which demonstrated identical amino acid coding (Table S1).

Experimental ECO/*pRHO-ABCA4* nanoparticles were prepared by self-assembly of ECO and the plasmid at a DNA concentration of 200 ng/μL and N/P ratio of 10 (Figure 4A). ECO/*pRHO-ABCA4* was subretinally injected at a dose of 200 ng in the right eye of the *Abca4*$^{-/-}$ mice with ECO/*pCMV-ABCA4* as a control. A substantial expression of *ABCA4* was observed in the retina at both mRNA and protein levels with ECO/*pRHO-ABCA4* 1 week after treatment (Figures 4B and 4C). *ABCA4* expression in retinas transfected with ECO/*pRHO-ABCA4* was 10-fold higher than in retinas transfected with ECO/*pCMV-ABCA4,* at the mRNA level. Immunofluorescence staining revealed specific expression of ABCA4 (Alexa488) in the photoreceptor outer segment of the retinas transfected with ECO/*pRHO-ABCA4* and ABCA4 expression in all retinal cell types with ECO/*pCMV-ABCA4*. The results demonstrated the capability of ECO/*pRHO-ABCA4* to produce efficient and specific ABCA4 expression in photoreceptor cells *in vivo*.

The efficacy of preventing Stargardt disease progression of gene therapy with ECO/*pRHO-ABCA4* was assessed based on the accumulation of A2E in the RPE in *Abca4*$^{-/-}$ mice. A2E, the photo-toxic dimers of vitamin A, is a main component of lipofuscin.[29,30] A2E accumulation is commonly used as an indicator of Stargardt disease progression.[31] One of the therapeutic strategies for treating Stargardt disease is to slow the production of A2E to minimize chronic oxidative damage that ultimately leads to atrophy. A2E accumulation gradually increased in *Abca4*$^{-/-}$ mice with aging (Figure S5). The *Abca4*$^{-/-}$ mice (1 month old) received a single subretinal injection of ECO/*pRHO-ABCA4* or ECO/*pCMV-ABCA4* with PBS as a control. Mice were euthanized at 6 months, and the A2E levels were analyzed

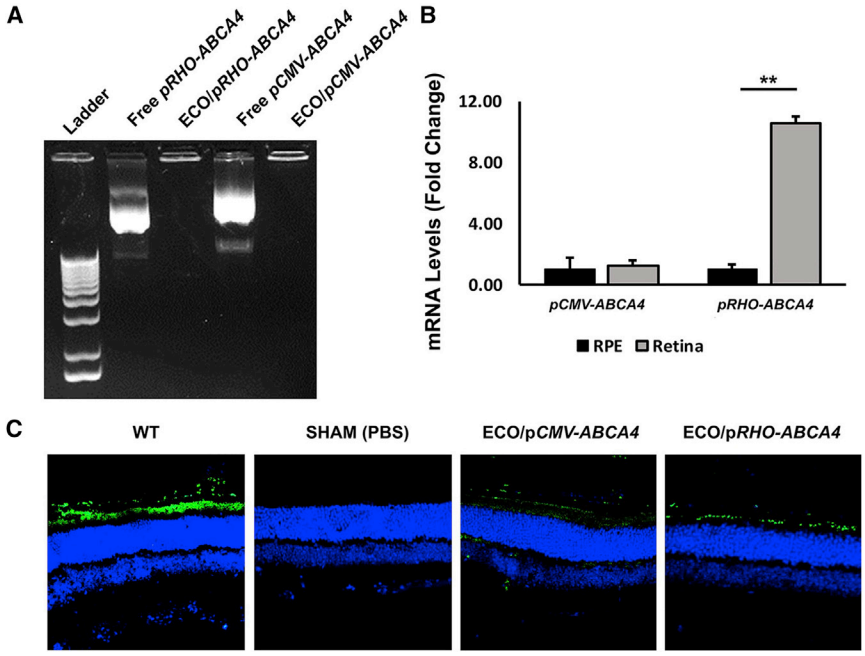

Figure 4. *In Vivo* Transfection Efficiency of ECO/*pRHO-ABCA4* and ECO/*pCMV-ABCA4* Nanoparticles in *Abca4*$^{-/-}$ Mice

(A–C) Gel electrophoresis of ECO/*pRHO-ABCA4* and ECO/*pCMV-ABCA4* nanoparticles (A); mRNA levels (B) and confocal images (C) of *ABCA4* expression (Alexa488) in the retina of *Abca4*$^{-/-}$ mice 7 days after subretinal injections of ECO/*pRHO-ABCA4* or ECO/*pCMV-ABCA4* nanoparticles with WT 129S1/SvImJ mice as control. ($n = 3$, $^{**}p < 0.005$. The mRNA level in the retina was normalized to the mRNA level in the RPE. Statistical analysis was conducted with two-tailed Student's t test.)

using high-performance liquid chromatography (HPLC) with the control as the contralateral eye (Figure 5A).

A2E was eluted from the HPLC column with an acetonitrile (ACN) (0.1% trifluoroacetic acid [TFA]) and water (0.1% TFA) gradient. The A2E level was determined by integration of the A2E peaks from the HPLC chromatograms. The ECO/*pRHO-ABCA4*-treated mice had a substantial A2E reduction when compared to controls and those treated with ECO/*pCMV-ABCA4*. Quantitative analysis showed an average of 35% A2E reduction in the ECO/*pRHO-ABCA4*-treated mice as compared to a 15% reduction in ECO/*pCMV-ABCA4*-treated mice (Figure 5B). Histochemical analysis of the retina revealed no significant differences in the retinal structure and integrity between the PBS and treated groups (Figure 5C), possibly due to the fact that the *Abca4*$^{-/-}$ mouse model did not demonstrate clear retinal degeneration within the treatment period.[32,33]

Substantial *ABCA4* expression was also observed in *Abca4*$^{-/-}$ mice treated with ECO/*pRHO-ABCA4* at the mRNA and protein levels 8 months after a single subretinal injection (Figure 6). ECO/*pRHO-ABCA4* resulted in a significantly greater *ABCA4* mRNA expression than ECO/*pCMV-ABCA4* when compared to PBS control, as shown by qRT-PCR. Immunofluorescence staining (Alexa488) revealed substantial ABCA4 protein expression in the photoreceptor outer segment section of the mice treated with ECO/*pRHO-ABCA4* (Figure 6B) as compared with the groups treated with ECO/*pCMV-ABCA4* and PBS. The ECO/*pABCA4* nanoparticles did not result in any significant effects in retinal function in wild-type (WT) mice as compared to PBS after subretinal injection, indicated by levels of electroretinogram (ERG) intensities (Figure S6). Based on the ERG results, any damage observed was attributed to the injection, not the injected substances. ECO/*pRHO-ABCA4* nanoparticles were demonstrated to be effective in mediating specific and prolonged *ABCA4* expression in *Abca4*$^{-/-}$ mice for the effective treatment of Stargardt disease.

DISCUSSION

One of the main challenges for gene therapy of Stargardt disease is the safe and efficient delivery and specific expression of the *ABCA4* gene in the photoreceptors. Both viral and non-viral approaches have been tested for treating Stargardt disease. Dual AAV strategies have been used to deliver two halves of the *ABCA4* gene to overcome the limited payload capacity of a single AAV.[13,14] Although dual AAVs have been shown to mediate expression of the full-length ABCA4 protein in the photoreceptor outer segment of *Abca4*$^{-/-}$ mice, they demonstrated low transduction efficiency and also induced the expression of truncated ABCA4.[14,34] Lentivirus has the capacity to deliver *ABCA4* gene stably and permanently in the transduced cells. Subretinal injection of lentivirus delivering *ABCA4* resulted in the significant expression of ABCA4 and reduction of A2E accumulation in *Abca*$^{-/-}$ mice.[35] Acceptable safety was demonstrated for the lentivirus despite the concern of uncontrolled integration into the genome and oncogenic effects of retroviruses.[36]

As compared to viral vectors, non-viral delivery systems have the advantages of unlimited payload, low immunogenicity, and minimal side effects.[17] The efficacy of non-viral delivery systems for treating Stargardt disease was first demonstrated by pegylated polylysine DNA nanoparticles with an interphotoreceptor retinoid-binding protein (IRBP) promoter or a mouse opsin promoter.[18] Subretinal injection of the nanoparticles resulted in the prolonged expression of ABCA4 protein, improved recovery of dark adaptation, and reduced lipofuscin accumulation in *Abca4*$^{-/-}$ mice. Despite the recent progress in non-viral gene delivery systems, there have not been any non-viral gene delivery systems that have been used in clinical trials for gene therapy of inherited retinal diseases. Thus, there remains a great need for safe and effective gene therapy, which could be addressed using highly efficient non-viral delivery systems.

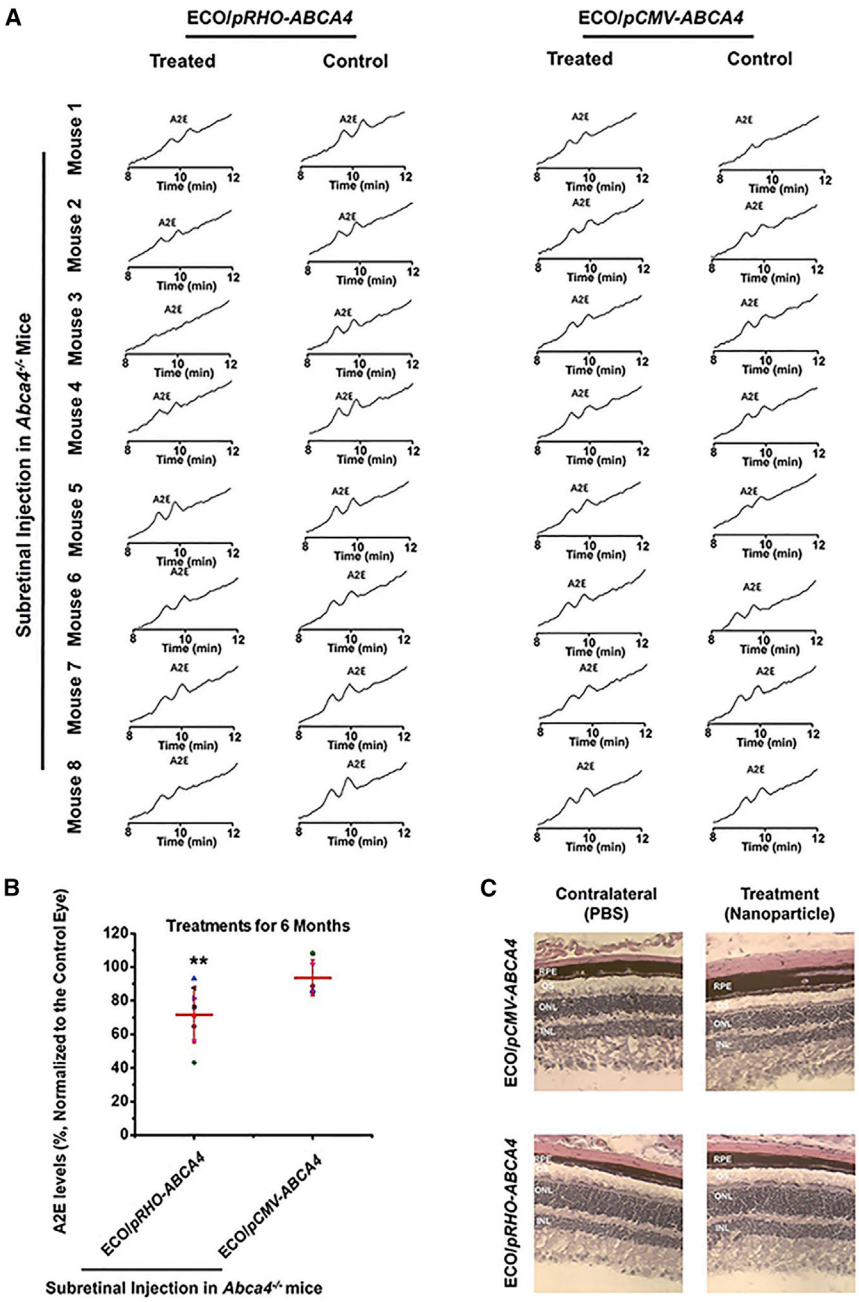

Figure 5. Efficacy of ECO/*pRHO-ABCA4* for Preventing A2E Accumulation in *Abca4*$^{-/-}$ Mice

(A and B) HPLC chromatograms (A) and relative quantity (B) of A2E extracted from the eyes of *Abca4*$^{-/-}$ mice treated with ECO/*pRHO-ABCA4* and ECO/*pCMV-ABCA4* with PBS as a control. (C) H&E staining of the retina after the treatments. (n = 8, error bars ± SD, **p < 0.05 relative to contralateral control eyes. Statistical analysis was conducted with two-tailed Student's t test.)

One of the main challenges for non-viral gene delivery systems is the cellular and subcellular barriers for gene transduction and prolonged gene expression in target cells. The multifunctional pH-sensitive cationic lipid ECO was designed as a gene carrier, with features of self-assembly formation of stable nanoparticles with *pDNA* without helper lipids, pH-sensitive amphiphilic cell membrane destabilization, and endosomal escape and reductive dissociation of the nanoparticles to release nucleic acids in the cytoplasm (PERC).[25,37] These features enable ECO to form stable nanoparticles with *pABCA4* at a low N/P ratio (Figure 1) and to sense and respond to environmental changes during the delivery process. In addition, these features help mediate efficient intracellular gene delivery and gene expression (Figure 2).

Another challenge of non-viral gene therapy for Stargardt disease is the specific prolonged expression of the therapeutic *ABCA4* gene in the outer segments of the photoreceptor cells. The therapeutic *ABCA4* plasmid was constructed with the bovine rhodopsin-specific promoter (RHO) to assure specific expression of ABCA4 in the outer segment. Compared to the CMV common constitutive promoter, selective expression of the reporter gene and therapeutic gene was achieved with the RHO promoter in wild-type mice and *Abca4*$^{-/-}$ mice (Figures 4 and 6). In addition, the tissue-specific RHO promoter has shown promise for long-term specific gene expression, while the viral CMV promoter often facilitates non-specific transient protein expression in mammalian cells.[38] As such, substantial *ABCA4* expression was observed for at least 8 months in the outer segment of the photoreceptor cells of *Abca4*$^{-/-}$ mice with ECO/*pRHO-ABCA4*, and no significant long-term gene expression for ECO/*pCMV-ABCA4* was seen (Figure 6). Minimizing off-target transgene expression with the tissue-specific promoter is also critical to improve the safety of gene therapy.[39]

The therapeutic efficacy of ECO/*pRHO-ABCA4* in treating Stargardt disease was demonstrated in *Abca4*$^{-/-}$ mice, a Stargardt disease animal model. *Abca4*$^{-/-}$ mice exhibited increased lipofuscin accumulation[40] (Figure S5), similar to the pathological observations in human Stargardt disease patients. Lipofuscin or A2E accumulation in the RPE is responsible for the pathological damage to the retina.[41,42] Inhibition or slowdown of A2E or lipofuscin accumulation is considered as the critical first step for preserving the retina and vision in effective treatment of Stargardt disease. Treatment with ECO/*pRHO-ABCA4* resulted in a significant reduction (35%) of A2E accumulation in *Abca4*$^{-/-}$ mice

6 months after a single injection as compared to the control-treated mice (Figure 5). This result is comparable to the treatment with a lentiviral gene delivery system for Stargardt disease.[35] In contrast, ECO/*pCMV-ABCA4* only produced about 15% A2E reduction. ECO/*pDNA* nanoparticles exhibited the same safety to the retina as PBS in wild-type mice after subretinal injection, based on the ERG analysis.

Future studies are necessary to optimize the ECO/*pDNA* nanoparticles to enhance ABCA4 expression and to improve therapeutic efficacy. Although it might be difficult for ECO/*pRHO-ABCA4* to induce the high level of ABCA4 expression as observed in the retina of the wild-type mice (Figure 4), enhanced gene expression with the non-viral approach would result in a further reduction of A2E accumulation. The *pRHO-ABCA4* construct could be modified to enhance gene expression efficiency in the photoreceptor outer segment. The formulation of ECO/*pRHO-ABCA4* nanoparticles could be optimized to improve intracellular transduction. Subretinal injection can also be improved to facilitate transfection of the photoreceptors across the retina. There was a relatively large variation in the reduction of A2E accumulation in the *Abca4*$^{-/-}$ mice treated with ECO/*pRHO-ABCA4* (Figure 5A). A high reduction of A2E accumulation was observed in some of the treated mice. The result indicates that improved therapeutic efficacy could be achieved by further optimization of the non-viral gene therapy. Recently, it was reported that ABCA4 expression was found in the mouse RPE cells, which was about 1% of the level in neural retina homogenates. This expression is at least part of the cause of the ocular *Abca4*$^{-/-}$ phenotype.[43] Therefore, RPE cells can be a potential target to rescue *abca4*-mediated retinal degenerations.

In conclusion, the self-assembled nanoparticles of multifunctional pH-sensitive amino lipid ECO and therapeutic *ABCA4* plasmid ECO/*pRHO-ABCA4* mediated specific and prolonged gene expression in the outer segment of the photoreceptors. There was a substantial reduction of A2E accumulation in the retina of *Abca4*$^{-/-}$ mice treated with the nanoparticles as compared to the controls. The nanoparticles also showed excellent safety profiles after subretinal injection. ECO/*pRHO-ABCA4* has the potential to overcome the limitations of AAV-based viral gene therapy for the effective treatment of Stargardt disease. The multifunctional lipid ECO plasmid DNA nanoparticles can be a promising non-viral gene therapy platform to deliver therapeutic genes of various sizes for treating a broader range of inherited retinal degenerations.

MATERIALS AND METHODS

Reagents

All reagents purchased from the vendors were used without further purification unless otherwise stated. TFA was purchased from Oakwood Products (West Columbia, SC, USA). Methylene chloride (DCM), chloroform, methanol, and acetonitrile were purchased from Fisher Scientific (Hampton, NH, USA). Lipofectamine 2000 and all reagents for cell culturing, including fetal bovine serum, streptomycin, and penicillin, were purchased from Invitrogen (Carlsbad, CA, USA). Reporter gene plasmids *pCMV-GFP* and *pRHO-DsRed* were purchased from Addgene repository (Addgene plasmids 11153 and 11156, respectively). *pCMV-ABCA4* was a gift from Robert S. Molday (University of British Columbia), and it contained the full-length human *ABCA4* cDNA sequence (NCBI: NM_000350.2) on a *pCEP4* backbone.

Cell Culture

ARPE-19 cells were cultured in DMEM and supplemented with 10% fetal bovine serum, 100 μg/mL streptomycin, and 100 U/mL penicillin (Invitrogen). Cells were maintained in a humidified incubator at 37°C and 5% CO_2.

Animals

The animals were housed and bred in the Animal Resource Center at Case Western Reserve University, and they were cared for according to an approved protocol by the Case Western Reserve University Institutional Animal Care and Use Committee (IACUC 2014-0053) and in compliance with recommendations from the American Veterinary Medical Association Panel on Euthanasia and the ARVO Statement for the Use of Animals in Ophthalmic and Vision Research.

Wild-type 129S1/SvImJ mice were purchased from Jackson Laboratory (Bar Harbor, ME, USA). Pigmented *Abca4*$^{-/-}$ knockout mice were generated as described previously[44] and maintained with either pigmented 129Sv/Ev or C57BL/6 mixed backgrounds, and their siblings were used for future experiments.

Plasmid Constructs

Plasmids were transformed in MAX Efficiency DH5α Competent *E. coli* (Life Technologies) and grown overnight on Luria-Bertani (LB) agar plates containing ampicillin. Selected colonies were amplified overnight and purified using a QIAGEN Plasmid Maxi Kit, according to the manufacturer's protocol. Plasmid purity and size were verified by gel electrophoresis. The *pRHO-ABCA4* plasmid was constructed by molecular cloning of the cDNA for the *ABCA4* gene into the linearized *pRHO-DsRed* plasmid, with the *DsRed* reporter gene removed. All enzymes were purchased from New England Biolabs (Ipswich, MA, USA). cDNA for the *ABCA4* gene was amplified by PCR with the Q5 High-Fidelity DNA Polymerase enzyme. The forward primer was 5′-AATACCG GTATGGGCTTCGTGAGACAGATA-3′ and the reverse primer was 5′-TATATAGCGGCCGCTAGCTCAGTCTGCTGTTT-3′ for adding the *AgeI* and *NotI* restriction sites to the 5′ and 3′ ends of *Abca4*, respectively. cDNA was purified using a QIAquick PCR Purification Kit (QIAGEN, Germantown, MD, USA) according to the manufacturer's instructions. The amplified *Abca4* cDNA and *pRHO-DsRed* plasmid were cut using the *NotI* and *AgeI* restriction endonucleases and purified by gel electrophoresis using the QIAGEN gel extraction kit, according to the manufacturer's instructions. Calf intestinal alkaline phosphatase (CIP) was added to the

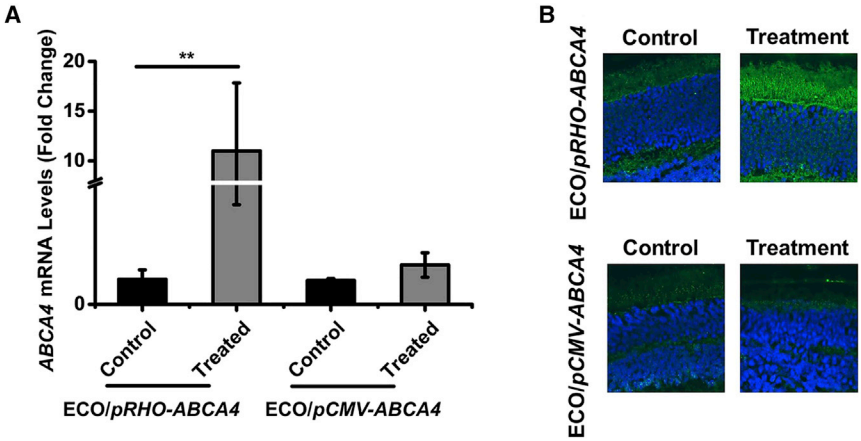

Figure 6. *ABCA4* Gene Expression Induced by ECO/*pRHO-ABCA4* Nanoparticles in *Abca4*$^{-/-}$ Mice at 8 Months

(A and B) *ABCA4* mRNA expression (A) and immunofluorescence confocal images (B) of ABCA4 expression the retinas were treated with ECO/*pRHO-ABCA4*, ECO/*pCMV-ABCA4*, and PBS. (n = 3, **p < 0.05. Statistical analysis was conducted with two-tailed Student's t test.)

endonuclease reaction with the *pRHO* vector to dephosphorylate vector termini and prevent self-annealing of the open ends. For the ligation step, the cut *pRHO* vector and *ABCA4* cDNA were incubated overnight at 16°C with the T4 DNA Ligase enzyme in the supplied reaction buffer. Ligation products were verified by gel electrophoresis and transformed and amplified. Final plasmid stocks were confirmed by Sanger sequencing.

Agarose Gel Electrophoresis

Plasmid construction products and nanoparticle formation were verified using agarose gel electrophoresis. Gels were made by heating 0.8%–2% agarose in 1× tris borate EDTA (TBE) buffer (Thermo Fisher Scientific, Waltham, MA, USA). While cooling, 1 μL ethidium bromide (EtBr) was added per 50 mL gel and poured into a gel mold to solidify. Samples were mixed with 6× purple DNA loading dye (New England Biolabs, Ipswich, MA, USA) prior to loading, and the leftmost lane was loaded with the 1 kb plus DNA ladder (Thermo Fisher Scientific). For cloning products, 80 V was applied for 80 min. For nanoparticles, 100 V was applied for 30 min. Gels were imaged using a ChemiDoc XRS+ gel imaging system (Bio-Rad, Hercules, CA, USA).

ECO/*pDNA* Nanoparticle Formulation

Lipid ECO was synthesized as previously described.[20,21] ECO/*pDNA* nanoparticles were prepared by self-assembly of ECO with plasmid DNA at an N/P ratio of 10. The ECO stock solution (2.5 mM in ethanol) and plasmid DNA stock solution (0.5 mg/mL) at predetermined amounts based on the N/P ratio were diluted into equal volumes with nuclease-free water, mixed, and shaken for 30 min at room temperature. A different ECO stock solution (25 mM) was used for *in vivo* formulations. Lipofectamine 2000/DNA nanoparticles were prepared according to the manufacturer's recommendation, which were formulated with 2 μL Lipofectamine 2000 and the *pDNA* amount was kept the same as the one in ECO/*pDNA* nanoparticles. Condensation of *pDNA* with ECO into nanoparticles was verified by agarose gel electrophoresis prepared in a 2% agarose gel run at 100 mV for 30 min. Size and zeta potential of the nanoparticles were determined using dynamic light scattering (DLS) with an Anton Paar Litesizer 500 (Anton Paar USA, Ashland, VA, USA). DLS measurements were performed at particle counts from 150∼400 kcounts/s. Relative frequency intensity weighted nanoparticle size distribution and zeta potential were recorded.

Transmission Electron Microscopy

The morphology of ECO/*pCMV-ABCA4* (N/P = 10) and Lipofectamine 2000/*pCMV-ABCA4* nanoparticles was imaged with a transmission electron microscope (JEOL JEM2200FS) (JEOL, Pleasanton, CA, USA). Samples for transmission electron microscopy (TEM) were prepared by depositing 20 μL particle solution onto a 300-mesh copper grid covered by a thin amorphous carbon film (20 nm). Immediately after deposition, the excess liquid was removed by touching the grid with filter paper. Samples were stained twice by adding 3 μL 2% uranyl acetate aqueous solution. The excess of staining solution was removed and nanoparticle images were acquired with TEM.

In Vitro Transfection

ARPE-19 cells were seeded onto 12-well plates at a density of 5×10^4 cells/well and allowed to grow for 24 h at 37°C. Transfections were conducted in 10% serum media with the ECO/*pDNA* nanoparticles at a DNA concentration of 1 μg/mL. ECO/*pDNA* nanoparticles were incubated with ARPE-19 cells for 4 h at 37°C. The media were then replaced with fresh serum-containing media (10% serum), and cells were then cultured for an additional 48 h. For reporter genes, GFP and DsRed expressions were evaluated with an Olympus FV1000 confocal microscope (Olympus, Center Valley, PA, USA). For the evaluation of *ABCA4* gene expression, qRT-PCR analysis was performed.

In Vivo Transfection

Subretinal injection was adapted from the Technical Briefs described by Timmers et al.[45] and Johnson et al.[46] Mice were anesthetized by intraperitoneal injection of a cocktail (15 μL/g body weight) comprising ketamine (6 mg/mL) and xylazine (0.44 mg/mL) in PBS buffer (10 mM sodium phosphate and 100 mM NaCl [pH 7.2]). Pupils were dilated with 1.0% tropicamide ophthalmic solution (Bausch & Lomb, Rochester, NY, USA). Following complete pupil dilation, filtered PBS was added dropwise and liberally to each eye,

and the residual liquid removed with gauze. Gonak Hypromellose Ophthalmic Demulcent Solution eye gel (Akorn, Lake Forest, IL, USA) was then added to each eye, and the mouse was positioned under a surgical microscope with its nose pointing toward the non-dominant hand of the surgeon. A 7-mm circular coverslip was placed over the cornea to observe the degree of pupil dilation and retinal vessels, and the coverslip was left on the eye to expedite ocular incision and injection. Curved forceps were used to separate the eyeball away from eyelids and socket. The cornea was carefully punctured temporally about 0.5 to 1 mm medial to the dilated pupillary margin with a 30G hypodermic needle (Becton Dickinson, Franklin Lakes, NJ, USA) with the bevel facing up. The needle was advanced through the cornea into the anterior chamber parallel to the anterior lens face.

After removing this needle, a 35G blunt needle connected to an RPE-KIT (World Precision Instruments, Sarasota, FL, USA) was inserted through the corneal incision and aimed slightly nasally toward the posterior chamber with the iris lateral and lens medial. The lens was displaced more medially as the needle was advanced into the posterior chamber. From this new position, the needle was located posterior to the lens in the posterior chamber, after avoiding the posterior lens and neural retina. With the syringe held in place, 1 μL ECO/*pDNA* nanoparticle solution was injected at a rate of 150 nL/s. Because intraocular pressure provides resistance to injected fluid, the needle was held in place for an extra 5 s to ensure complete injection. Successful administration was confirmed by bleb formation. Triple antibiotic ophthalmic ointment (neomycin, polymyxin, and bacitracin) was administered after injections, and the eyelids were manually closed to promote recovery. The mouse was kept on the warming pad until awake, then transferred to its home cage until analysis. In reporter gene experiments, equimolar amounts of ECO/*pCMV-GFP* and ECO/*pRHO-DsRed* formulations were mixed together prior to injection, and 100 ng of each plasmid was delivered. In gene replacement therapy, 200 ng of either *pCMV-ABCA4* or *pRHO-ABCA4* was delivered. PBS (1 μL) was injected to the contralateral eye as control. At least 3 days following injections, the retinal structure was imaged by optical coherence tomography to confirm that the injection site had healed and the retina had not detached.

qRT-PCR

Cell lysis and homogenization in cell lines were performed using a cell scraper in lysis buffer. For animal tissues, mice were sacrificed and eyes enucleated. Eyecups were dissected in PBS buffer and retinas and RPEs were separated. Tissues were homogenized manually using a glass rod in lysis buffer. RNA extraction was performed using a QIAGEN RNeasy kit, according to the manufacturer's instructions. mRNA transcripts were converted to cDNA using the miScriptII reverse transcriptase kit (QIAGEN, Germantown, MD, USA). qRT-PCR was performed with SYBR Green Master mix (AB Biosciences, Allston, MA, USA) in an Eppendorf Mastercycler machine. Fold changes were normalized to 18S, with SHAM eyes as controls.

Electroretinography

Wild-type 129S1/SvImJ mice were injected with PBS, ECO/*pCMV-ABCA4*, or ECO/*pRHO-ABCA4* as described above. Full-field electroretinograms were acquired according to a previous method[47] at day 7 and day 30. Animals were anesthetized and pupils dilated according to the same procedure as for subretinal injections. Mice were dark-adapted for at least 2 days prior to ERG recording, and recording experiments were performed in a dark room. Three electrodes were placed on the mouse: a contact lens electrode on each eye, a reference electrode under the skin between the ears, and a ground underneath the skin of the tail. ERGs were recorded with a UTAS E-3000 electrophysiologic recording system (LKC Technologies, Gaithersburg, MD, USA). Mice were placed in a dark chamber and scotopic and photopic responses to flash stimuli were obtained from both eyes simultaneously. Flash stimuli were at the intensity of 1.6 $\log(cd \cdot s \cdot m^{-2})$, and white light flash duration was 10 ms. Illumination-response curves were recorded and scotopic and photopic a and b waves were calculated.

Synthesis and HPLC Analysis of A2E

A mixture of all-*trans*-retinal (100 mg, 352 μmol) and ethanolamine (9.5 mg, 155 μmol) in ethanol (3.0 mL) was stirred in the presence of acetic acid (9.3 μL, 155 μmol) at room temperature with a sealed cap in the dark for 2 days. After the mixture was concentrated *in vacuo*, the residue was purified by silica gel column chromatography. After elution with MeOH:CH_2Cl_2 (5:95), further elution with MeOH:CH_2Cl_2:trifluoroacetic acid (8:92:0.001) gave A2E. Pure samples were obtained by HPLC purification (ZORBAX 300 SB-C18, 9.4 × 250 mm, 84%–100% water/acetonitrile for 30 min, and 1.0 mL/min flow detected at UV 430 nm). A2E was detected at retention time (t_R = 35.2 min). Collection of the fraction provided pure A2E for further analysis. A2E was characterized by mass spectrometry.

For A2E analysis from tissue, mice were euthanized by cervical dislocation and eyes were excised with curved scissors. The eyes were deep-frozen in liquid nitrogen immediately after removal and stored at −80°C until used. A2E was extracted from the eyes of each mouse in 1 mL acetonitrile after homogenization with a Brinkmann Politron homogenizer (Kinematica, Lucerne, Switzerland). After evaporation of solvent, extracts were dissolved in 120 μL acetonitrile with 0.1% TFA and then filtered through a Teflon syringe filter. Samples (100 μL) were loaded on a C18 column (ultrasphere ODS, 4.6 × 250 mm) (Beckman Coulter, Indianapolis, IN, USA) and analyzed by reverse-phase HPLC. A2E was eluted with the following gradients of acetonitrile in water (containing 0.1% trifluoroacetic acid): 85%–96% (10 min), 96% (5 min), 96%–100% (2 min), and 100% (13 min) (flow rate, 1 mL/min), and they were monitored at 430 nm. For A2E quantitation by reverse-phase HPLC, the area of the A2E peak was normalized to the synthesized A2E standard.

Immunohistochemistry

To assess gene expression and distribution throughout the retina, eyecups were prepared for histological analysis as previously

published.[19] Mice were sacrificed by cervical dislocation, and the eyes were enucleated and washed in PBS buffer prior to fixation in 4% paraformaldehyde (PFA) in PBS buffer. After 2 h, the eyecups were removed and fixed in 4% PFA overnight. The next day, samples were transferred to 20% sucrose/optical cutting temperature (OCT) (Tissue-Tek optimal cutting temperature compound, Sakura, Torrance, CA, USA) via a gradual sucrose gradient. The eyecups were incubated in 20% sucrose/OCT overnight, and then imbedded in cryomolds and frozen in OCT. Frozen slides were cut in 10-μm-thick slices and adhered to glass slides. Prior to immunohistochemistry, slides were warmed to room temperature and washed in Tris-buffered saline with 1% Tween 20 (TBST) buffer. Heat-induced antigen retrieval was conducted in 10 mM citrate buffer (pH 6.0) in a pressure cooker for 20 min, and slides were allowed to slowly cool to room temperature. Primary antibodies used for immunohistochemistry (IHC) were rabbit anti-GFP for GFP, rabbit polyclonal anti-RFP (Cat #600-401-379, Rockland, Limerick, PA, USA) for DsRed, and the mouse monoclonal 3F4 (Cat #NBP130032, Abcam, Cambridge, MA, USA) for ABCA4. Fluorescent secondary antibodies were donkey anti-rabbit or anti-mouse immunoglobulin G (IgG) Alexa488 (Cat #715-545-151, Jackson ImmunoResearch Laboratories, West Grove, PA, USA), and these slides were imaged using an Olympus FV1000 confocal microscope (Olympus, Center Valley, PA, USA).

Statistical Analysis

The *in vitro* experiments were performed in triplicate. The numbers of mice for *in vivo* experiments are listed in the captions. The data are presented as the means and SDs. Statistical analysis was conducted with ANOVA and two-tailed Student's t tests using a 95% confidence interval. Statistical significance was accepted when $p \leq 0.05$.

SUPPLEMENTAL INFORMATION

Supplemental Information can be found online at https://doi.org/10.1016/j.ymthe.2019.09.010.

AUTHOR CONTRIBUTIONS

Z.-R.L. conceived the project. D.S. and R.M.S. were involved in all aspects of this work. A.E.S. performed subretinal injections. S.-Q.G. performed ERG examinations. A.V. performed qRT-PCR analysis. W.S. performed gene sequencing. Z.H., R.M.S., and D.S. performed cloning. A.M., T.K., and K.P. provided assistance with animal models and experiment design. All authors read and approved the final paper.

CONFLICTS OF INTEREST

The authors declare no competing interests.

ACKNOWLEDGMENTS

This project was supported by the Gund-Harrington Scholars Award from the Harrington Discovery Institute and the Foundation of Fighting Blindness, NEI R24-EY-024864 and R24-EY-027283, the Canadian Institute for Advanced Research (CIFAR), and Alcon Research Institute (ARI). Z.-R.L. is an M. Frank Rudy and Margaret Domiter Rudy Professor of Biomedical Engineering. K.P. is the Leopold Chair of Ophthalmology.

REFERENCES

1. Boye, S.E., Boye, S.L., Lewin, A.S., and Hauswirth, W.W. (2013). A comprehensive review of retinal gene therapy. Mol. Ther. *21*, 509–519.
2. Allikmets, R., Shroyer, N.F., Singh, N., Seddon, J.M., Lewis, R.A., Bernstein, P.S., Peiffer, A., Zabriskie, N.A., Li, Y., Hutchinson, A., et al. (1997). Mutation of the Stargardt disease gene (*ABCR*) in age-related macular degeneration. Science *277*, 1805–1807.
3. Tsybovsky, Y., Molday, R.S., and Palczewski, K. (2010). The ATP-binding cassette transporter ABCA4: structural and functional properties and role in retinal disease. In Inflammation and Retinal Disease: Complement Biology and Pathology, J.D. Lambris and A.P. Adamis, eds. (Springer New York), pp. 105–125.
4. Chen, Y., Okano, K., Maeda, T., Chauhan, V., Golczak, M., Maeda, A., and Palczewski, K. (2012). Mechanism of all-trans-retinal toxicity with implications for stargardt disease and age-related macular degeneration. J. Biol. Chem. *287*, 5059–5069.
5. Koenekoop, R.K. (2003). The gene for Stargardt disease, ABCA4, is a major retinal gene: a mini-review. Ophthalmic Genet. *24*, 75–80.
6. Puntel, A., Maeda, A., Golczak, M., Gao, S.-Q., Yu, G., Palczewski, K., and Lu, Z.R. (2015). Prolonged prevention of retinal degeneration with retinylamine loaded nanoparticles. Biomaterials *44*, 103–110.
7. Charbel Issa, P., Barnard, A.R., Herrmann, P., Washington, I., and MacLaren, R.E. (2015). Rescue of the Stargardt phenotype in *Abca4* knockout mice through inhibition of vitamin A dimerization. Proc. Natl. Acad. Sci. USA *112*, 8415–8420.
8. Schwartz, S.D., Regillo, C.D., Lam, B.L., Eliott, D., Rosenfeld, P.J., Gregori, N.Z., Hubschman, J.P., Davis, J.L., Heilwell, G., Spirn, M., et al. (2015). Human embryonic stem cell-derived retinal pigment epithelium in patients with age-related macular degeneration and Stargardt's macular dystrophy: follow-up of two open-label phase 1/2 studies. Lancet *385*, 509–516.
9. Lenis, T.L., Sarfare, S., Jiang, Z., Lloyd, M.B., Bok, D., and Radu, R.A. (2017). Complement modulation in the retinal pigment epithelium rescues photoreceptor degeneration in a mouse model of Stargardt disease. Proc. Natl. Acad. Sci. USA *114*, 3987–3992.
10. Wright, J.F., Wellman, J., and High, K.A. (2010). Manufacturing and regulatory strategies for clinical AAV2-hRPE65. Curr. Gene Ther. *10*, 341–349.
11. Conlon, T.J., Deng, W.-T., Erger, K., Cossette, T., Pang, J.J., Ryals, R., Clément, N., Cleaver, B., McDoom, I., Boye, S.E., et al. (2013). Preclinical potency and safety studies of an AAV2-mediated gene therapy vector for the treatment of MERTK associated retinitis pigmentosa. Hum. Gene Ther. Clin. Dev. *24*, 23–28.
12. Russell, S., Bennett, J., Wellman, J.A., Chung, D.C., Yu, Z.-F., Tillman, A., Wittes, J., Pappas, J., Elci, O., McCague, S., et al. (2017). Efficacy and safety of voretigene neparvovec (AAV2-hRPE65v2) in patients with RPE65-mediated inherited retinal dystrophy: a randomised, controlled, open-label, phase 3 trial. Lancet *390*, 849–860.
13. McClements, M.E., Barnard, A.R., Singh, M.S., Charbel Issa, P., Jiang, Z., Radu, R.A., and MacLaren, R.E. (2019). An AAV Dual Vector Strategy Ameliorates the Stargardt Phenotype in Adult *Abca4*$^{-/-}$ Mice. Hum. Gene Ther. *30*, 590–600.
14. Trapani, I., Toriello, E., de Simone, S., Colella, P., Iodice, C., Polishchuk, E.V., Sommella, A., Colecchi, L., Rossi, S., Simonelli, F., et al. (2015). Improved dual AAV vectors with reduced expression of truncated proteins are safe and effective in the retina of a mouse model of Stargardt disease. Hum. Mol. Genet. *24*, 6811–6825.
15. Dyka, F.M., Boye, S.L., Chiodo, V.A., Hauswirth, W.W., and Boye, S.E. (2014). Dual adeno-associated virus vectors result in efficient in vitro and in vivo expression of an oversized gene, MYO7A. Hum. Gene Ther. Methods *25*, 166–177.
16. Lopes, V.S., and Williams, D.S. (2015). Gene Therapy for the Retinal Degeneration of Usher Syndrome Caused by Mutations in MYO7A. Cold Spring Harb. Perspect. Med. *5*, a017319.
17. Glover, D.J., Lipps, H.J., and Jans, D.A. (2005). Towards safe, non-viral therapeutic gene expression in humans. Nat. Rev. Genet. *6*, 299–310.
18. Han, Z., Conley, S.M., Makkia, R.S., Cooper, M.J., and Naash, M.I. (2012). DNA nanoparticle-mediated ABCA4 delivery rescues Stargardt dystrophy in mice. J. Clin. Invest. *122*, 3221–3226.
19. Sun, D., Sahu, B., Gao, S., Schur, R.M., Vaidya, A.M., Maeda, A., Palczewski, K., and Lu, Z.R. (2017). Targeted Multifunctional Lipid ECO Plasmid DNA Nanoparticles as

Efficient Non-viral Gene Therapy for Leber's Congenital Amaurosis. Mol. Ther. Nucleic Acids *7*, 42–52.

20. Malamas, A.S., Gujrati, M., Kummitha, C.M., Xu, R., and Lu, Z.-R. (2013). Design and evaluation of new pH-sensitive amphiphilic cationic lipids for siRNA delivery. J. Control. Release *171*, 296–307.
21. Gujrati, M., Malamas, A., Shin, T., Jin, E., Sun, Y., and Lu, Z.-R. (2014). Multifunctional cationic lipid-based nanoparticles facilitate endosomal escape and reduction-triggered cytosolic siRNA release. Mol. Pharm. *11*, 2734–2744.
22. Parvani, J.G., Gujrati, M.D., Mack, M.A., Schiemann, W.P., and Lu, Z.-R. (2015). Silencing β3 Integrin by Targeted ECO/siRNA Nanoparticles Inhibits EMT and Metastasis of Triple-Negative Breast Cancer. Cancer Res. *75*, 2316–2325.
23. Sun, D., Maeno, H., Gujrati, M., Schur, R., Maeda, A., Maeda, T., Palczewski, K., and Lu, Z.R. (2015). Self-Assembly of a Multifunctional Lipid With Core-Shell Dendrimer DNA Nanoparticles Enhanced Efficient Gene Delivery at Low Charge Ratios into RPE Cells. Macromol. Biosci. *15*, 1663–1672.
24. Gujrati, M., Vaidya, A., and Lu, Z.-R. (2016). Multifunctional pH-Sensitive Amino Lipids for siRNA Delivery. Bioconjug. Chem. *27*, 19–35.
25. Sun, D., Schur, R.M., and Lu, Z.-R. (2017). A novel nonviral gene delivery system for treating Leber's congenital amaurosis. Ther. Deliv. *8*, 823–826.
26. Ho, S.C.L., Mariati, Yeo, J.H., Fang, S.G., and Yang, Y. (2015). Impact of using different promoters and matrix attachment regions on recombinant protein expression level and stability in stably transfected CHO cells. Mol. Biotechnol. *57*, 138–144.
27. Wiszniewski, W., Zaremba, C.M., Yatsenko, A.N., Jamrich, M., Wensel, T.G., Lewis, R.A., and Lupski, J.R. (2005). ABCA4 mutations causing mislocalization are found frequently in patients with severe retinal dystrophies. Hum. Mol. Genet. *14*, 2769–2778.
28. Zhang, N., Tsybovsky, Y., Kolesnikov, A.V., Rozanowska, M., Swider, M., Schwartz, S.B., Stone, E.M., Palczewska, G., Maeda, A., Kefalov, V.J., et al. (2015). Protein misfolding and the pathogenesis of ABCA4-associated retinal degenerations. Hum. Mol. Genet. *24*, 3220–3237.
29. Radu, R.A., Mata, N.L., Bagla, A., and Travis, G.H. (2004). Light exposure stimulates formation of A2E oxiranes in a mouse model of Stargardt's macular degeneration. Proc. Natl. Acad. Sci. USA *101*, 5928–5933.
30. Kennedy, C.J., Rakoczy, P.E., and Constable, I.J. (1995). Lipofuscin of the retinal pigment epithelium: a review. Eye (Lond.) *9*, 763–771.
31. Radu, R.A., Mata, N.L., Nusinowitz, S., Liu, X., Sieving, P.A., and Travis, G.H. (2003). Treatment with isotretinoin inhibits lipofuscin accumulation in a mouse model of recessive Stargardt's macular degeneration. Proc. Natl. Acad. Sci. USA *100*, 4742–4747.
32. Weng, J., Mata, N.L., Azarian, S.M., Tzekov, R.T., Birch, D.G., and Travis, G.H. (1999). Insights into the function of Rim protein in photoreceptors and etiology of Stargardt's disease from the phenotype in *abcr* knockout mice. Cell *98*, 13–23.
33. Charbel Issa, P., Barnard, A.R., Singh, M.S., Carter, E., Jiang, Z., Radu, R.A., Schraermeyer, U., and MacLaren, R.E. (2013). Fundus autofluorescence in the *Abca4*$^{(-/-)}$ mouse model of Stargardt disease–correlation with accumulation of A2E, retinal function, and histology. Invest. Ophthalmol. Vis. Sci. *54*, 5602–5612.
34. Trapani, I., Colella, P., Sommella, A., Iodice, C., Cesi, G., de Simone, S., Marrocco, E., Rossi, S., Giunti, M., Palfi, A., et al. (2014). Effective delivery of large genes to the retina by dual AAV vectors. EMBO Mol. Med. *6*, 194–211.
35. Kong, J., Kim, S.R., Binley, K., Pata, I., Doi, K., Mannik, J., Zernant-Rajang, J., Kan, O., Iqball, S., Naylor, S., et al. (2008). Correction of the disease phenotype in the mouse model of Stargardt disease by lentiviral gene therapy. Gene Ther. *15*, 1311–1320.
36. Binley, K., Widdowson, P., Loader, J., Kelleher, M., Iqball, S., Ferrige, G., de Belin, J., Carlucci, M., Angell-Manning, D., Hurst, F., et al. (2013). Transduction of photoreceptors with equine infectious anemia virus lentiviral vectors: safety and biodistribution of StarGen for Stargardt disease. Invest. Ophthalmol. Vis. Sci. *54*, 4061–4071.
37. Wang, X.-L., Ramusovic, S., Nguyen, T., and Lu, Z.-R. (2007). Novel polymerizable surfactants with pH-sensitive amphiphilicity and cell membrane disruption for efficient siRNA delivery. Bioconjug. Chem. *18*, 2169–2177.
38. Gill, D.R., Pringle, I.A., and Hyde, S.C. (2009). Progress and prospects: the design and production of plasmid vectors. Gene Ther. *16*, 165–171.
39. Yin, H., Kanasty, R.L., Eltoukhy, A.A., Vegas, A.J., Dorkin, J.R., and Anderson, D.G. (2014). Non-viral vectors for gene-based therapy. Nat. Rev. Genet. *15*, 541–555.
40. Radu, R.A., Yuan, Q., Hu, J., Peng, J.H., Lloyd, M., Nusinowitz, S., Bok, D., and Travis, G.H. (2008). Accelerated accumulation of lipofuscin pigments in the RPE of a mouse model for ABCA4-mediated retinal dystrophies following Vitamin A supplementation. Invest. Ophthalmol. Vis. Sci. *49*, 3821–3829.
41. Brunk, U.T., and Terman, A. (2002). Lipofuscin: mechanisms of age-related accumulation and influence on cell function. Free Radic. Biol. Med. *33*, 611–619.
42. Terman, A., and Brunk, U.T. (1998). Lipofuscin: mechanisms of formation and increase with age. APMIS *106*, 265–276.
43. Lenis, T.L., Hu, J., Ng, S.Y., Jiang, Z., Sarfare, S., Lloyd, M.B., Esposito, N.J., Samuel, W., Jaworski, C., Bok, D., et al. (2018). Expression of ABCA4 in the retinal pigment epithelium and its implications for Stargardt macular degeneration. Proc. Natl. Acad. Sci. USA *115*, E11120–E11127.
44. Maeda, A., Maeda, T., Golczak, M., and Palczewski, K. (2008). Retinopathy in mice induced by disrupted all-trans-retinal clearance. J. Biol. Chem. *283*, 26684–26693.
45. Timmers, A.M., Zhang, H., Squitieri, A., and Gonzalez-Pola, C. (2001). Subretinal injections in rodent eyes: effects on electrophysiology and histology of rat retina. Mol. Vis. *7*, 131–137.
46. Johnson, C.J., Berglin, L., Chrenek, M.A., Redmond, T.M., Boatright, J.H., and Nickerson, J.M. (2008). Technical brief: subretinal injection and electroporation into adult mouse eyes. Mol. Vis. *14*, 2211–2226.
47. Schur, R.M., Sheng, L., Sahu, B., Yu, G., Gao, S., Yu, X., Maeda, A., Palczewski, K., and Lu, Z.R. (2015). Manganese-Enhanced MRI for Preclinical Evaluation of Retinal Degeneration Treatments. Invest. Ophthalmol. Vis. Sci. *56*, 4936–4942.